The Potassium Promoter Function in the Oxidation of Graphite: An Experimental and Theoretical Study

Christoph Janiak,[†,‡] Roald Hoffmann,[*,†] Peter Sjövall,[§] and Bengt Kasemo[*,§]

Department of Chemistry and Materials Science Center, Cornell University, Ithaca, New York 14853-1301, and Department of Physics, Chalmers University of Technology, S-41296 Göteborg, Sweden

Received January 15, 1993. In Final Form: September 7, 1993[⊗]

The interaction of potassium and oxygen, individually and as coadsorbates with graphite, was studied experimentally and theoretically. In the experiments the sticking of oxygen was investigated at different K coverages. The extremely low sticking coefficient for chemisorption/dissociation of dioxygen on clean graphite is contrasted by the high sticking coefficient for even very dilute potassium overlayers. KO_2 and K_2O complexes are identified as early precursors to CO_2 formation from coadsorbed potassium and oxygen. The K–O complexes formed on the surface and their transformations (as a function of increasing temperature) were followed by thermal desorption spectroscopy (TDS) and electron energy loss spectroscopy (HREELS). A theoretical study based on the tight-binding method indicates why the presence of potassium facilitates the chemisorption of dioxygen, whose sticking coefficient on clean graphite is otherwise very small. It is suggested that the potassium promotion effect is a very local one and that formation of a $K–O_2$ surface complex is the first step in graphite oxidation. The strongly preferred adsorption site for O_2 on a K-covered surface is on top of a potassium atom with no interaction to the graphite layer. From there the dioxygen molecule can dissociate into oxygen atoms. The stabilizing $K–O_2$ interaction can be traced to a localized sp-hybrid available for bonding to O_2 and the fact that the graphite π system is not distorted upon chemisorption of O_2 via the potassium spacer. Concerning the favored adsorption sites for the individual species, a slight preference is deduced for K above a hexagon (6-fold symmetry site), while O and O_2 more strongly favor a position on top of a carbon atom (O_2 in a bent end-on approach) for the undamaged surface. Surface defects, however, figure prominently in stabilizing the oxygen species and also a potassium atom in the defect area.

Introduction

Chemical reactions of solid carbon with oxygen, water, and carbon dioxide, known as carbon gasification reactions, have attracted considerable interest in the last decades, mainly because of their relevance in energy technology.[1] It is well established that these reactions are catalyzed by, e.g., alkali salts and transition-metal oxides added to the carbon substrate.[2]

The reactive properties of solid surfaces are often dramatically modified by adsorption of alkali metals.[3] It is a well-known phenomenon that potassium, or more generally, alkali metals can catalyze a myriad of reactions of gaseous substances with surfaces. Experimental observations of this phenomenon are available over the range from semiconductor (e.g. Si, GaAs)[4] through semimetal (carbon in the from of graphite or charcoal)[5–7] to metal[3,8] or metal oxide[9] surfaces, interacting with dioxygen, water, carbon monoxide, carbon dioxide, etc. Subsequently, this effect is exploited in a wide range of technological applications, e.g. in heterogeneous catalysis[10] and semiconductor oxidation.[11,12] The gasification of coal and charcoal is promoted for over a century by additives such as caustic soda (NaOH) or lime (CaO).[2,13–15] Enhancement of reactivity by alkali metals has stimulated extensive experimental and also theoretical studies.

Various mechanisms have already been proposed for the catalytic effects of alkali additives in the form of *alkali metal salts* (e.g. carbonates) in the gasification of carbonaceous materials.[16–18] The catalytic effect of alkali *compounds* in carbon gasification reactions is often explained in terms of a mechanism referred to as the oxygen transfer mechanism.[2,16] According to this mechanism, the active catalyst undergoes sequential oxidation–reduction cycles on the carbon surface. Oxygen from the gas phase thus is captured on the surface by direct reaction with the catalyst. Subsequent reduction of the catalyst provides oxygen atoms, which react with the carbon surface to form CO and CO_2. This mechanism has received experimental support and is usually favored over the so-called electron transfer mechanism.[2] In the latter mechanism, the adsorbed alkali is assumed to cause strengthening of

† Cornell University.

‡ Present address: Institut für Anorganische und Analytische Chemie, Technische Universität Berlin, Strasse des 17 Juni 135, D-10623 Berlin, Germany.

§ Chalmers University of Technology.

⊗ Abstract published in *Advance ACS Abstracts*, October 15, 1993.

(1) Laurendeau, N. M. *Prog. Energy Combust. Sci.* **1978**, *4*, 221.
(2) McKee, D. W. *Chem. Phys. Carbon* **1981**, *16*, 1.
(3) Bonzel, H. P. *Surf. Sci. Rep.* **1987**, *8*, 43.
(4) Starnberg, H. I.; Soukiassian, P.; Bakshi, M. H.; Hurych, Z. *Surf. Sci.* **1989**, *224*, 13.
(5) Sjövall, P.; Hellsing, B.; Keck, K.-E.; Kasemo, B. *J. Vac. Sci. Technol.* **1987**, *A5*, 1065.
(6) Sjövall, P.; Hellsing, B.; Keck, K.-E.; Kasemo, B. *Mat. Res. Soc. Symp. Proc.* **1988**, *111*, 447.
(7) (a) Sams, D. A.; Shadman, F. *AIChE J.* **1986**, *32*, 1132. (b) Wen, W.-Y. *Catal. Rev.-Sci. Eng.* **1980**, *22*, 1.
(8) Aruga, T.; Murata, Y. *Prog. Surf. Sci.* **1989**, *31*, 61.
(9) O'Young, C.-L. *J. Phys. Chem.* **1989**, *93*, 2016.
(10) (a) Ertl, G.; Weiss, M.; Lee, S. B. *Chem. Phys. Lett.* **1979**, *60*, 391. (b) Campbell, C. T.; Goodman, D. W. *Surf. Sci.* **1982**, *123*, 413. (c) Mross, W.-D. *Catal. Rev.-Sci. Eng.* **1983**, *25*, 591.
(11) (a) Soukiassian, P.; Gentle, T. M.; Bakshi, M. H.; Bommannavar, A. S.; Hurych, Z. *Phys. Scr.* **1987**, *35*, 757.
(12) Oellig, E. M.; Michel, E. G.; Asensio, M. C.; Miranda, R. *Appl. Phys. Lett.* **1987**, *50*, 1660.
(13) See the special issue of *Fuel* **1983**, *62* (2), 140–262, which contains the papers presented at a symposium on Fundamentals of Catalytic Coal and Carbon Gasification.
(14) Kelemen, S. R.; Freund, H. *J. Catal.* **1986**, *102*, 80.
(15) Cabrera, A. L.; Heinemann, H.; Somorjai, G. *J. Catal.* **1982**, *75*, 7.
(16) (a) McKee, D. W. *Fuel* **1983**, *62*, 170. (b) Wood, B. J.; Sancier, K. M. *Catal. Rev.-Sci. Eng.* **1984**, *26*, 233.
(17) Mims, C. A.; Pabst, J. K. *Fuel* **1983**, *62*, 176.
(18) Moulijn, J. A.; Cerfontain, M. B.; Kapteijn, F. *Fuel* **1984**, *63*, 1043, and references therein.

0743-7463/93/2409-3427$04.00/0

carbon–oxygen bonds and weakening of the carbon–carbon bonds as a result of electron transfer to the carbon substrate.

The influence of alkali *metal* adsorption on the surface properties of metals, graphite (semimetal), and semiconductors is related to the electropositive nature of the alkali metals which can easily donate their single valence electron to the "surface". In the physicist's language, alkali adsorption causes a charge redistribution on the surface that effectively gives rise to a dipole field which lowers the work function of the surface.[3,8,19] The so-called promoting effect of alkali metals in surface reactions is often discussed in terms of this (local) charge redistribution and work function decrease.[20]

In a previus experimental study by two of us[5,6] we observed that the oxidation rate of evaporated carbon can be greatly enhanced—by up to 10^4 times—through a predeposited potassium layer. A theoretical model had also been proposed[5] which showed that the large rate increase upon K adsorption could be explained by a K-induced increase in the dissociation rate for the O_2 molecules impinging on the surface, due to a more effective coupling between the O_2 antibonding π^* orbital and the occupied π states in the K-promoted graphite. In other words, a lower work function of K-graphite is proposed to result in more charge/electron transfer to O_2, especially its half-filled π^* level. This in turn increases the dissociation probability of O_2, eventually leading to chemisorption of atomic oxygen.[5,21,22] For metal surfaces a work function decrease is known to affect the adsorption kinetics and the sticking coefficient of dioxygen.[3]

There is also an "oxygen-transfer mechanism", the essence of this model being that O_2 reacts directly with K and then the KO_x complex is reduced by carbon atoms in the surface. Several chemical forms of the active potassium catalyst have been suggested for the oxygen transfer based reaction mechanisms. The potassium oxides, K_2O, K_2O_2, and KO_2, are obvious candidates, because they can undergo oxidation–reduction cycles by transformation between the different oxidation states.[2,16,23] Mims and Pabst were able to detect the presence of a surface complex on the carbon surface during gasification conditions.[17] Schlögl suggested that the presence of potassium hydroxide, KOH, on the carbon surface is essential for the catalytic effect,[24] while other reaction schemes include potassium carbonate, K_2CO_3, as an intermediate.[2,16] In all these experimental studies, however, the potassium catalyst was added in the form of KOH or K_2CO_3.

Thus, the alkali-catalyzed dioxygen–carbon reaction still presents some unsettled questions: It remains a matter of controversy whether or not the promotion effect is *local* or *nonlocal*.[5,25] *Local* is here taken to mean that the potassium atom is a direct participant in the reaction and that it undergoes an oxidation–reduction sequence. *Nonlocal* implies that the increased reactivity of O_2 is due solely to an electronic influence that the alkali metal has on the carbon substrate. Combinations of these mechanisms are, of course, also possible.

Concerning the mechanism of catalytic carbon oxidation, an important problem is to determine the chemical identity of the potassium catalyst under oxidation conditions. The electron transfer mechanism would be favored if atomic or intercalated potassium were present in the carbon substrate, since these potassium configurations are expected to cause large electron transfer to the carbon substrate.[16] Atomic and intercalated potassium are, however, not thermally stable in the graphite substrate at gasification temperatures.[14,26] Thus, it seems unlikely that these forms of potassium are important for the catalytic effect in carbon gasification.

The "potassium-on-graphite" problem is further related to alkali–graphite intercalation compounds[27] and to studies of other metal atoms (e.g. Cu, Ag, Au, Al,[28] or Pt[29]) on graphite. The *chemi*sorption of the oxygen molecule (O_2) on graphite/K is related to the adsorption of O_2 on semiconductors[4] or metals,[30] O_2 (and also N_2[31]) *physi*sorption on graphite,[32,33] and to the oxygen atom (O[34] and also N, H,[35–37] H_2O,[38] NO, CO, etc.[39]) chemisorption on graphite and other main group elements (semiconductors).[40] The distinction between molecular dioxygen (O_2) and atomic oxygen (O) is significant; the two species differ in their chemical behavior. While atomic oxygen apparently requires very little activation energy to react with a clean graphite surface with a high probability, molecular dioxygen reacts only at high temperature with a much smaller probability and surface defects are said to be important for the reactions.[41] The dioxygen–graphite surface *chemi*sorption is suggested to be *endo*thermic.[34,42] The binding energy of *physi*sorbed O_2, on the other hand, is about 0.1 eV, i.e. exothermic. (For the distinction between chemi- and physisorption, see below).

The experimental studies referred to above[5,6] have been extended to thermal desorption spectroscopy (TDS)

(19) Heskett, D.; Maeda Wong, T.; Smith, A. J.; Graham, W. R.; DiNardo, N. J.; Plummer, E. W. *J. Vac. Sci. Technol.* **1989**, *B7*, 915.
(20) (a) Nørskov, J. K.; Holloway, S.; Lang, N. D. *Surf. Sci.* **1984**, *137*, 65. (b) Lang, N. D.; Holloway, S.; Nørskov, J. K. *Surf. Sci.* **1985**, *150*, 24. (c) Feibelman, P. J.; Hamann, D. R. *Surf. Sci.* **1985**, *149*, 48.
(21) Franciosi, A.; Soukiassian, P.; Philip, P.; Chang, S.; Wall, A.; Raisanen, A.; Troullier, N. *Phys. Rev. B* **1987**, *35*, 910.
(22) Hellsing, B. *Phys. Rev. B* **1989**, *40*, 3855.
(23) Saber, J. M.; Falconer, J. L.; Brown, L. F. *J. Catal.* **1984**, *90*, 65.
(24) Schlögl, R. In *Physics and Chemistry of Alkali Metal Adsorption*; Bonzel, H. P.; Bradshaw, A. M.; Ertl, G., Eds.; Elsevier: Amsterdam, 1989.
(25) Albano, E. V. *Surf. Sci.* **1989**, *215*, 333.
(26) Sjövall, P.; Kasemo, B. To be submitted for publication.
(27) (a) Rüdorff, W.; Schulze, E. *Z. Anorg. Allg. Chem.* **1954**, *277*, 156. (b) Rüdorff, W. *Adv. Inorg. Chem. Radiochem.* **1959**, *1*, 223. (c) Inoshita, T.; Nakao, K.; Kamimura, H. *J. Phys. Soc. Jpn.* **1977**, *43*, 1237. (d) Lagrange, P.; Guerard, D.; Herold, A. *Ann. Chim. Fr.* **1978**, *3*, 143. (e) Dresselhaus, M. S.; Dresselhaus, G. *Adv. Phys.* **1981**, *30*, 139. (f) DiVincenzo, D. P.; Rabii, S. *Phys. Rev. B* **1982**, *25*, 4110. (g) Loupias, G.; Codazzi, V.; Rabii, S.; Tatar, R. C.; Ascone, I.; Guerard, D.; Elansari, L. *Synth. Met.* **1989**, *34*, 411. (h) Ohno, T.; Nakao, K.; Kamimura, H. *J. Phys. Soc. Jpn.* **1979**, *47*, 1125.
(28) Ganz, E.; Sattler, K.; Clarke, J. *Surf. Sci.* **1989**, *219*, 33.
(29) Eppell, S.; Chottiner, G. S.; Scherson, D. A.; Pruett, G. *Langmuir* **1990**, *6*, 1316.
(30) Roberts, M. W. *Chem. Soc. Rev.* **1989**, *18*, 451, and references therein.
(31) (a) Wang, S.-K.; Newton, J. C.; Wang, R.; Taub, H.; Dennison, J. R. *Phys. Rev. B* **1989**, *39*, 10331. (b) Barone, V.; Lelj, F.; Ioaconis, E.; Illas, F.; Russo, N. *J. Mol. Struct. (Theochem)* **1986**, *139*, 277.
(32) (a) Toney, M. F.; Fain, S. C., Jr. *Phys. Rev. B* **1987**, *36*, 1248. (b) Mochrie, S. G. J.; Sutton, M.; Akimitsu, J.; Birgeneau, R. J.; Horn, P. M.; Dimon, P.; Moncton, D. E. *Surf. Sci.* **1984**, *138*, 599. (c) Toney, M. F.; Diehl, R. D.; Fain, S. C., Jr. *Phys. Rev. B* **1983**, *27*, 6413. (d) Heiney, P. A.; Stephens, P. W.; Mochrie, S. G. J.; Akimitsu, J.; Birgeneau, R. J.; Horn, P. M. *Surf. Sci.* **1983**, *125*, 539. (e) Pan, R. P.; Etters, R. D.; Kobashi, K.; Chandrasekharan, V. *J. Chem. Phys.* **1982**, *77*, 1035. (f) Stoltenberg, J.; Vilches, O. E. *Phys. Rev. B* **1980**, *22*, 2920. (g) Nielsen, M.; McTague, J. P. *Phys. Rev. B* **1979**, *19*, 3096.
(33) Youn, H. S.; Hess, G. B. *Phys. Rev. Lett.* **1990**, *64*, 443.
(34) Barone, V.; Lelj, F.; Iaconis, E.; Illas, F.; Russo, N.; Jounou, A. *J. Mol. Struct. (Theochem.)* **1986**, *136*, 313.
(35) (a) Mendoza, C.; Ruette, F. *Catal. Lett.* **1989**, *3*, 89. (b) Chen, J. P.; Yang, R. T. *Surf. Sci.* **1989**, *216*, 481. (c) Barone, V.; Lelj, F.; Minichino, C.; Russo, N.; Toscano, M. *Surf. Sci.* **1987**, *189/190*, 185. (d) Bennett, A. J.; McCaroll, B.; Messmer, R. P. *Phys. Rev. B* **1971**, *3*, 1397.
(36) LaFemina, J. P.; Lowe, J. P. *J. Am. Chem. Soc.* **1986**, *108*, 2527.
(37) Dovesi, R.; Pisani, C.; Ricca, F.; Roetti, C. *J. Chem. Phys.* **1976**, *65*, 3075.
(38) Miura, K.; Morimoto, T. *Langmuir* **1988**, *4*, 1283.
(39) Russo, N.; Toscano, M. *J. Mol. Struct. (Theochem)* **1989**, *201*, 149.
(40) Zheng, X. M.; Cao, P. L. *Surf. Sci.* **1989**, *219*, L543.
(41) Wong, C.; Yang, R. T.; Halpern, B. L. *J. Chem. Phys.* **1983**, *78*, 3325.
(42) Zarif Yanz, Y. A.; Kiselev, V. F.; Lezhnev, N. N.; Nikitina, D. V. *Carbon* **1967**, *5*, 127.

studies of K and CO_2 desorption after initial adsorption of O_2, at 136 K, and to vibrational spectroscopic studies of the K_xO_y complexes formed on the surface. The results most relevant to the present study are presented below. More detailed results are given elsewhere.[43-45]

Previous studies have shown that the probability for dissociative adsorption of O_2 molecules impinging on a clean carbon surface, leading to the formation of CO and CO_2, is very low, at least $<10^{-3}$ at room temperature, and that the process is thermally activated.[46,47] Furthermore, the reaction probability is very sensitive to the surface structure and strongly influenced by defects. For example, the sticking coefficient for O_2 on a clean graphite surface at 673 K increased from $<10^{-14}$ to 10^{-7} when a graphite surface with low defect concentration was damaged by Ar^+ bombardment.[46] At very low temperatures molecular oxygen is physisorbed on graphite. The monolayer desorption temperature is 47 K.[48]

It seems generally accepted that the sticking and dissociation of dioxygen is frequently the bottleneck of surface oxidation reactions.[4]

Note: When referring to the "graphite surface", we generally mean the basal or 0001 plane of graphite.

Experimental Methods and Procedures

The experimental details have been described elsewhere.[2,5,43] In short the experiments were performed in an ultrahigh vacuum (UHV) system with a base pressure in the low 10^{-10} Torr range. The system is equipped with a CMA Auger electron spectrometer for surface purity control and for work function measurements, with a high resolution electron energy loss spectrometer (HREELS) for vibrational spectroscopy, and with a mass spectrometer for thermal desorption spectroscopy. Low energy electron diffraction (LEED) is used for surface crystal structure control.

The sample was oriented graphite, exposing the basal plane. The sample was cleaned by heating, initially for several hours at 1200 K. Potassium was deposited from a break-seal glass ampule[43] or from an alkali metal getter source.[2] Oxygen exposures were normally made in the 10^{-8} Torr range by backfilling the chamber with oxygen.

Experimental Results

The results are presented in a condensed form with special emphasis on observations of relevance to the theoretical calculations. For additional information see refs 43-45. On the clean graphite surface no oxygen adsorption (sticking coefficient $<10^{-3}$–10^{-4}) was observed down to 136 K, and no reaction to form CO or CO_2 was observed in O_2 atmospheres up to 10^{-5} Torr and 700 K. This finding is consistent with earlier work,[40,41,45,46] indicating no or very weak dioxygen chemisorption and a large activation barrier for O_2 dissociation.

In contrast the O_2 sticking coefficient on potassium-covered graphite is unity or close to unity, even at very dilute potassium coverages.[43] The initial sticking coefficient is constantly near unity, at least down to a potassium coverage of 5% of a full monolayer (Figure 1). This behavior can be explained[5,43] either in terms of a direct interaction of O_2 with the graphite surface, modified by electron donation from adsorbed potassium, or as a precursor adsorption[45c] of O_2 into the physisorbed state,[48] where it eventually reacts with potassium atoms on the surface. In the former case the mechanism is a direct charge transfer to the O_2 molecule impinging on the surface, enhanced by the lowered work function and possibly also by the increased electron density at the Fermi level.[5] In the second case the reaction occurs as a direct reaction between a weakly perturbed, physisorbed O_2 molecule and potassium atoms on the graphite surface. The theoretical analysis below will elucidate these questions.

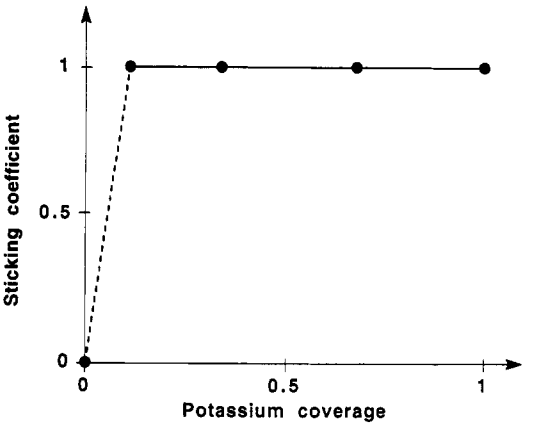

Figure 1. Sticking coefficient of O_2 on potassium-covered graphite as a function of potassium coverage.

As a consequence of O_2 sticking on the potassium-covered surface, various K–O complexes are formed, as revealed by the HREELS spectra (Figure 2A, for details see ref 45a,b). At least three different species are observed with vibrational energies around 27, 31, and 39–41 meV. The 31-meV peak is not obvious in Figure 2A, the spectrum at 160 K, but clearly identifiable at different exposure and coverage conditions.[45b]

At low temperatures, the vibrational loss peaks are fairly broad, indicating heterogeneous broadening (i.e. there is a mixture of local stoichiometries due to kinetic barriers). As the structures formed at low temperature are annealed, the peaks sharpen and undergo transformations. Some of these transformations are accompanied by desorption of potassium and/or CO_2 (Figure 2B). An additional factor influencing the surface K/O stoichiometry is potassium intercalation,[44,45] accompanying potassium deposition and annealing of the different K–O coadsorbate layers. By variation of the surface stoichiometry (i.e. the potassium/oxygen ratio), and guided by recent XPS/HREELS results from O_2 adsorption on potassium,[49] the loss peak at 39 meV is assigned to K_2O (for the detailed assignments, see ref 45a). The loss peak at 31 meV is especially pronounced at oxygen-rich conditions and is attributed to KO_2 or possibly K_2O_2.

The loss peak at 27 meV appears only after annealing of the K–O coadsorbates to 700 K, which then causes considerable desorption of potassium (Figure 2B). A definitive assignment is yet lacking. It is interesting to note that this is the only loss peak remaining after annealing to 700 K. Combining this observation with the CO_2 desorption occurring around 750 K (Figure 2B) leads to the conclusion that the 27-meV loss peak represents a precursor to CO_2 formation. It is tempting to speculate about the possibility of a carbonate species, but the lack of evidence for a C–O stretch vibrational does not at present provide any support for this hypothesis. (A C–O bond parallel to the surface would, however, escape detection by dipole scattering, so the existence of a CO bond cannot be excluded.)

(43) Sjövall, P.; Kasemo, B. *J. Chem. Phys.* **1993**, *98*, 5932.
(44) Sjövall, P.; Kasemo, B. *Surf. Sci.*, in press.
(45) (a) Chakarov, D.; Sjövall, P.; Kasemo, B. *J. Phys.: Condens. Matter* **1993**, *5*, 2903. (b) Chakarov, D.; Österlund, L.; Kasemo, B. To be submitted for publication. (c) Zhdanov, V. P.; Kasemo, B. Submitted for publication in *Chem. Phys.*
(46) Barber, M.; Evans, E. L.; Thomas, J. M. *Chem. Phys. Lett.* **1973**, *18*, 423.
(47) Marchon, B.; Carrazza, J.; Heinemann, H.; Somorjai, G. A. *Carbon* **1988**, *26*, 507.
(48) You, H.; Fain, S. C., Jr. *Phys. Rev. B* **1986**, *33*, 5886.
(49) Baddorf, A. P.; Itchkawitz, B. S. *Surf. Sci.* **1992**, *264*, 73.

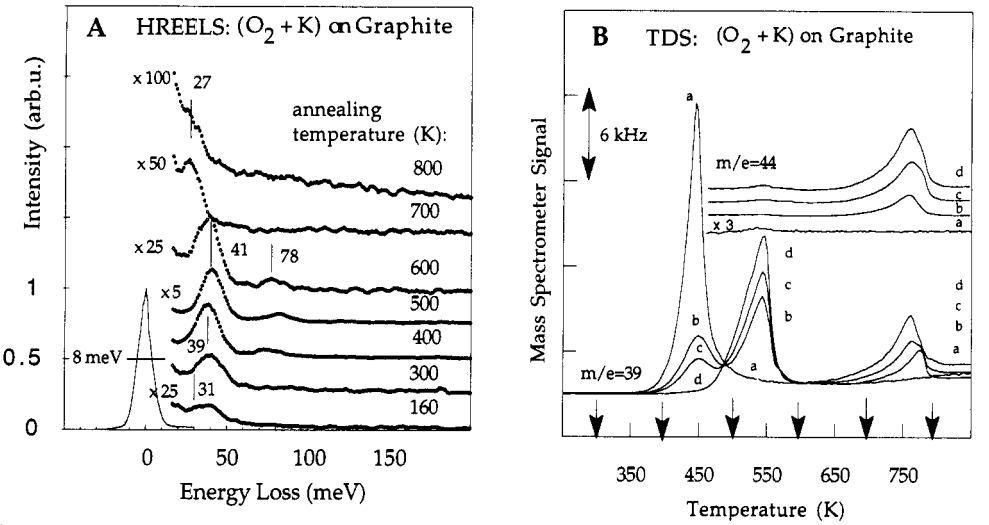

Figure 2. (A) HREEL spectra after 25 langmuirs O_2 exposure of 2.5 monolayers (ML) potassium on graphite and after annealing the surface to the indicated temperatures in vacuum. All spectra are recorded at 160 K. Primary electron energy 15 eV, specular scattering. The elastic peak shown corresponds to the unannealed system. (B) Thermal desorption spectra of potassium, m/e = 39, and carbon dioxide, m/e = 44, (a) after 1.2 ML deposition of potassium at 160 K on graphite, and after 3 (b), 8 (c), and 25 langmuirs (d) oxygen exposures at 160 K. Linear heating rate of 2.5 K·s^{-1}. The spectra for CO_2 are shifted upward for the sake of clarity. The CO_2 spectrum (a) is multiplied by a factor of 3. The arrows correspond to the annealing temperatures in Figure 2A.

The thermal desorption spectra (Figure 2B) contain desorption peaks for K and CO_2. The K peak around 450 K corresponds to metallic (unreacted) potassium, the peak at 500–550 K is due to potassium stabilized by oxygen, and the peak around 750–800 K is coninciding with CO_2 desorption.

By combining TDS and HREELS results, the following picture emerges. At low temperatures oxygen sticks on the potassium-covered surface with unity or nearly unity sticking even at low K coverages. At low potassium coverage the *average* K:O ratio at saturation is about 1:1, as judged from the sticking and TDS experiments, but due to intercalation the *surface* ratio is probably smaller. At high K coverage the saturation ratio is 2:1, indicating K_2O formation, and in agreement with the HREELS data. At low temperatures, kinetic barriers give rise to a mixture of stoichiometries.

Upon annealing, the surface K–O complexes go through a number of transformations. At temperatures up to 300–400 K, segregation of intercalated potassium increases the surface K:O ratio. At even higher temperatures some potassium desorbs from the surface, and as a result more oxygen-rich complexes are formed. Eventually total decomposition/reaction occurs to form CO_2 and desorbing K. The precursor species to CO_2 formation is associated with the 27-meV vibrational energy,[45] but its composition is yet unidentified. In mixed oxygen isotope experiments complete isotopic mixture is observed, among product CO_2 molecules,[44] indicating complete dissociation of dioxygen.[47]

The observations above point to the key role of dissociation of oxygen and potassium bonding to graphite and of K–O and C–O bonds on the surface. These are central questions in the theoretical analysis below.

Theoretical Preparations

The extensive experimental research in the area of graphite–adsorbate interactions has also generated a wealth of theoretical studies. Most of the calculations do not employ an extended, two-dimensional surface, but use cluster models instead.[35,38] To our best knowledge the actual chemisorption of O_2 on graphite, however, has only been studied once by theoretical methods. We want to contribute a chemcial perspective to this problem. Our calculations make use of the tight-binding extended Hückel method on an infinite, two-dimensional surface.[50]

Before we can embark on a full scale calculation, some decisions need to be made.

A One- or Two-Layer Slab? In many studies the graphite surface is simulated with a planar C_xH_y cluster model, an annulene system. In tight-binding calculations one graphite layer is typically used.[35–37,51] A one-layer annulene or graphite-net system is reasonable, since the interlayer distance in graphite of 335 pm is close to a van der Waals contact.

The effect of going from a one-layer to a two-layer slab is for the most part negligible, as our calculations show.[52] However, the introduction of a second layer leads to an inequivalency of the two carbon atoms within the surface unit cell. One carbon atom has a carbon directly underneath in the next layer (α site), whereas the other one is located above the center of a carbon hexagon in the next layer (β site)—illustrated in 1.

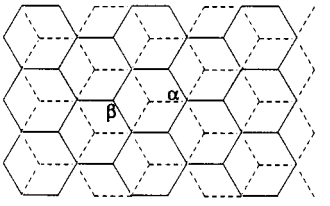

1

In an STM (scanning tunneling microscopy) picture of the basal plane of graphite, three carbon atoms of the hexagon appear much brighter than the other three, with the bright and not so bright spots alternating.[28,53–55] The brightest spots were assigned to the β sites, since calcu-

(50) Hoffmann, R. *Solid and Surfaces: A Chemist's View of Bonding in Extended Structures*, VCH: New York, 1988.

(51) (a) Perkins, P. G.; Marwaha, A. K.; Stewart, J. J. P. *Theor. Chim. Acta* **1980**, *57*, 1. (b) Messmer, R. P.; McCarroll, B.; Singal, C. M. *J. Vac. Sci. Technol.* **1972**, *9*, 891.

(52) Note, however, that two vs one graphite layer makes a difference in the total (integrated) DOS at the Fermi level. The one layer model results in a so-called zero band gap semiconductor, i.e. zero state density at ϵ_f, while the three-dimensional calculations yield a small overlap between the valence and conduction bands, resulting in a nonzero DOS at ϵ_f.

(53) Wiesendanger, R.; Anselmetti, D.; Geiser, V.; Hidber, H. R.; Güntherodt, H.-J. *Synth. Met.* **1989**, *34*, 175.

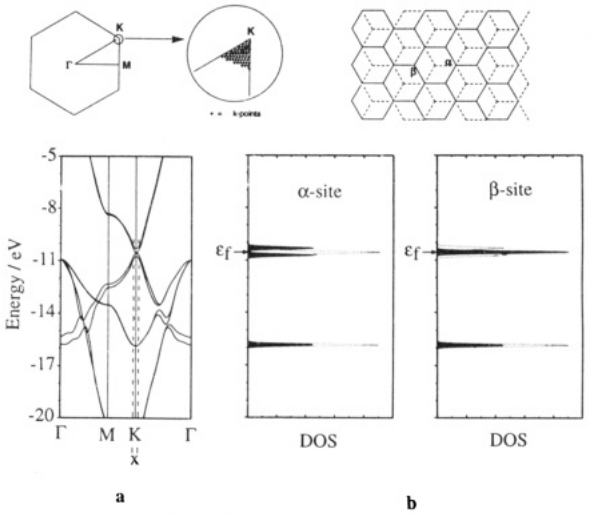

Figure 3. Partial band structure diagram (a) of a two-layer graphite slab. Density of state (DOS) plots (b) for a small region around K (denoted by X, within dashed lines in a, or see circled area with enlargement in the drawing of the Brillouin zone, above). The DOS plots show the total DOS (dotted lines) and projected DOS for the α- and β-site carbons (shaded area). 81 k points were used for this average property calculation.

lations showed these to have a higher electronic density of states (DOS) near the Fermi level—which is observed by STM—than the α sites.[54-56] However, recent STM studies of intercalated graphites[57] and single graphitic sheets on metal surfaces[58] argue against this interpretation. Also, it could not be completely ruled out that other effects might contribute to these huge STM corrugations, such as surface layer slippage and elastic deformations induced by the close proximity of the tunneling tip.[59] The origin of the unusual graphite STM images is still a matter of controversy;[54,60,61] one of us has recently done a thorough study of the problem, suggesting the possibility of charge and spin density waves[61] playing a role in the observed graphite STM images.

With our calculations we do not see any difference in the density of states for α and β sites when we average over the whole Brillouin zone. Only if we concentrate on the fraction of the surface Brillouin zone near the Fermi level, near special k-point K,[56] (illustrated in **2**) can we discriminate between the two different carbon atoms.

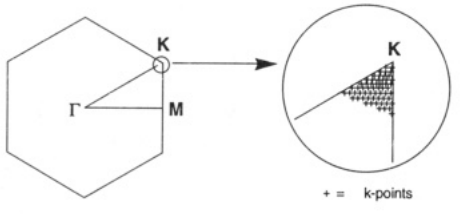

2

Figure 3 shows the DOS plots for the α and β sites from a small region around K. We see that the β sites clearly have the higher DOS right at the Fermi level—in agreement with the other computational results mentioned above. Focusing on the region around K in our calculation is necessary since not all k points in the Brillouin zone contribute to the charge densities sensed by STM—only k points around the Fermi level do. For typical tunneling voltages below 1 V[56] the portion of the band structure sampled by STM near the Fermi surface is very small; the Fermi level lies close to the special point K. For a simple, pedagogically effective approach to the π-band crystal orbitals and their degeneracy lifting in two- and three-dimensional graphites near the Fermi energy; see ref 62.

To return to the question posed at the beginning of this section, we conclude that it would be fairly safe to use only one graphite layer to model the surface. The inequivalencies between the two different carbon sites do not show up in a two-layer slab, neither on a bare surface nor with adsorbates attached to it. However, a two-layer slab allows for more options for simulation of defects (holes) in the surface which are important for the reactivity of graphite. Therefore, we opted for a two-layer slab.

Choice of Unit Cell for Chemisorption Studies. Potassium-promoted oxidation of graphite using pure potassium has been observed and studied experimentally for potassium submonolayer to monolayer coverages[5,6] (see experimental section). We need a unit cell large enough to treat submonolayer coverages. This is mostly the range explored experimentally and also the one of primary interest for the theoretical work. Larger coverages are expected to represent metallic potassium rather than potassium on graphite. Actually alkali-metal overlayers are frequently reported to become metallic somewhere above 0.1 monolayer coverage,[63,64] reflecting the large effective radius of the alkali metal.[6] For potassium, the minimum metal–metal separation in its elemental body centered cubic structure is 454.4 ppm.[65] Exactly where the metallic character of the alkali overlayer is well established can be debated and most likely depends on the substrate. For example, the plasmon frequency and work function characteristic of metallic K is not established until coverages higher than 0.1 ML, typically around 0.5 ML.

We tried to simulate a low-enough coverage throughout our calculations by selecting a large unit cell (cf. ref 36; concept of a molecular unit cell[51]). Our choice was a unit cell of 18 carbon atoms per layer (or 36 C's for the two layer slab) as depicted in **3**. The area spanned by this unit cell is about 4.7×10^{-15} cm^2. With an approximated monolayer coverage of 5×10^{14} K-atoms per cm^2,[3] one alkali-metal per unit cell then corresponds to a ~40% or 0.4 monolayer coverage. Note again, that here a monolayer or fraction thereof is referred to a close packed potassium layer and has no correspondence to the graphite structure, due to the incommensurate nature of the carbon and potassium atomic radii.

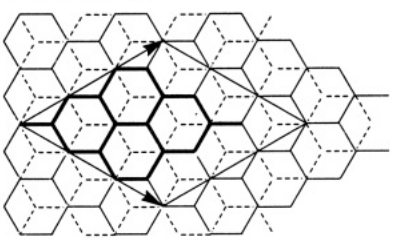

3

We are now ready to embark on our actual surface–adsorbate calculations, which might provide us with an

(54) Batra, I. P.; Garcia, N.; Rohrer, H.; Salemink, H.; Stoll, E.; Ciraci, S. *Surf. Sci.* **1987**, *181*, 126.
(55) Tománek, D.; Louie, S. G.; Mamin, H. J.; Abraham, D. W.; Thomson, R. E.; Ganz, E.; Clarke, J. *Phys. Rev. B* **1987**, *35*, 7790.
(56) Tománek, D.; Louie, S. G. *Phys. Rev. B* **1988**, *37*, 8327.
(57) (a) Kelty, S. P.; Lieber, C. M. *J. Phys. Chem.* **1989**, *93*, 5983. (b) Kelty, S. P.; Lieber, C. M. *Phys. Rev. B* **1989**, *40*, 5856.
(58) J. C. Hemminger, to be submitted for publication.
(59) Tersoff, J.; Lang, N. D. *Phys. Rev. Lett.* **1990**, *65*, 1132.
(60) Lawunmi, D.; Payne, M. C. *J. Phys.: Condens. Matter* **1990**, *2*, 3811.
(61) Tchougreeff, A. L.; Hoffmann, R. *J. Phys. Chem.* **1993**, *97*, 8993.
(62) LaFemina, J. P.; Lowe, J. P. *Int. J. Quantum Chem.* **1986**, *30*, 769.

understanding of the alkali-promoted oxidation of graphite. Specifically, we would like to find the preferred adsorption site for potassium and to understand the reason for the low sticking coefficient of dioxygen on a bare graphite surface, so as to comprehend the role of the potassium catalyst in enhancing the sticking and O_2 dissociation. The latter should help us to comment on the local *versus* nonlocal controversy discussed in the introduction and suggest some possible reaction mechanisms. Finally, we also want to explore how defects in the basal plane of graphite may influence its reactivity toward oxygen.

The Preferred Potassium Adsorption Site. On a graphite slab one can have four higher symmetry sites for a monoatomic adsorbate: (**A**) the "3-fold on-top site" directly above a carbon atom. Since the carbon atom can be an α or β carbon, as described earlier, we can, in principle, distinguish between an **A**α or an **A**β site. One may also envisage (**B**) the "2-fold bridging site" above the center of a carbon–carbon bond and (**C**) the "6-fold hollow site" above the center of a hexagon. The different sites are illustrated in **4**.

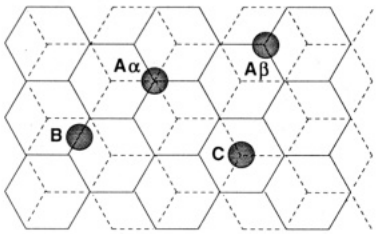

4

In this section we use an approximate molecular orbital method, the extended Hückel tight-binding procedure. This one-electron method gives only qualitative results but lends itself to the construction of simple explanations. Quantities computed by the extended Hückel methodology should be viewed as relative indications of stability of bonding.

In particular, the extended Hückel method is not expected to give reliable results as far as bond length variations are concerned. Therefore, we chose a C–K distance of 303 pm, based on structural studies of K–graphite intercalation compounds[27] (305 pm found), $[\eta^5\text{-}(PhCH_2)_5C_5]K(thf)_3$[66a] (average 303.5 pm; thf = tetrahydrofuran), $[\eta^5\text{-}(Me_3Si)C_5H_4]K$[66b] (average 300 pm), and $[\eta^5\text{-}Me_5C_5]K(pyridine)_2$[66c] (average 303 pm). This C–K distance was kept constant throughout our studies. We only note that in potassium–fluorenyl systems[67] the K–C distances are longer (range 307–332 pm) and vary more than in potassium–cyclopentadienyl complexes[66] (maximal variation there 296–310 pm).

Table I compares the binding energy, the charge on K, and the C–K overlap population for the four adsorption sites given in **4**. As expected (from what is known of graphite–potassium intercalation compounds and molecular cyclopentadienyl systems), the η^6-**C** site (6-fold hollow) is the most stable one for the potassium adsorbate. It not only has the highest binding energy but also gives the largest potassium–graphite overlap population, the latter

Table I. Comparison between Different Potassium Adsorption Sites on Graphite As Illustrated in 4

site[a]	E_b, binding energy/eV[b]	charge on potassium	C–K overlap population[c]
Aα	6.14	+0.62	0.055
Aβ	6.14	+0.62	0.055
B	6.18	+0.81	0.049 (×2)
C	6.40	+0.83	0.032 (×6)

[a] See **4** for illustration; C–K distance fixed at 303 pm. [b] $E_b = E$(bare graphite unit cell) + E(free K) − E(surface + adsorbate) = (−2556.708 eV) + (−4.34 eV) − E(surface + adsorbate), positive is surface-adsorbate complex more stable; Note that E_b is defined relative to a free K 4s energy of −4.34 eV. The single absolute value of E_b depends critically on the potassium parameters (see Appendix), so that only the trend noted here is of physical significance. [c] Overlap population to *one* carbon at a distance of 303 pm from the potassium. For the **B** site there are two; for **C** there are six carbons at this distance. To obtain a relative measure of the K–graphite bond strength, the C–K overlap population should be multiplied by this number of neighboring carbons as indicated in parentheses.

reflecting qualitatively the bond strength. In this hollow position the potassium can also transfer its electron most effectively to the graphite surface. The difference in the Fermi energy between the different adsorption sites (not shown in the table) is negligible. The small variation in binding energies for different adsorption site may indicate that it is easy for the potassium to move around on the graphite surface. The near identity of the **A**α and β sites is no surprise, after what we saw for the α and β sites for a bare grahite surface.

We note that this finding of a 6-fold hollow site-preference for K is different than what has been observed experimentally for the coinage metals and aluminum. The coinage metals—Cu, Ag, and Au—have a similar valence configuration, namely $d^{10}s^1$, to the alkali metals. However, STM studies show they prefer **A** and **B** sites.[28] Chemically, from a comparison with cyclopentadienyl model compounds, this does not come as a surprise: Cp–Cu^I, –Ag^I, or –Au^I complexes exhibit a σ-bonded, η^1-Cp–metal coordination, rather than a π-, η^5-bonding mode.

What we did not look at was the stability of the 6-fold potassium adsorption site with respect to alkali metal clustering. A strong tendency toward formation of metal adlayer islands at low coverages (about 1% of a metal monolayer) has been observed experimentally in STM studies of Cu, Ag, Au, and Al.[28] However, the potassium adsorption is accompanied by a larger charge transfer. Coulomb repulsion would then tend to keep the positively polarized K adsorbates apart at low coverages.

The Preferred Dioxygen Site on Bare Graphite. There is much geometrical freedom in the way diatomic O_2 can interact with the graphite surface. Relative to the surface plane the O–O bond vector might be (1) "side-on" (**5**), aligned parallel to the surface plane, (2) linear "end-on" (**6**), perpendicular to the surface plane, or (3) bent "end-on" (**7**), the vector forming an angle γ with the normal to the surface plane. "Side-on" and "linear, end-on" are, of course, special positions (γ = 90 and 180°) of the general case shown in **7**.

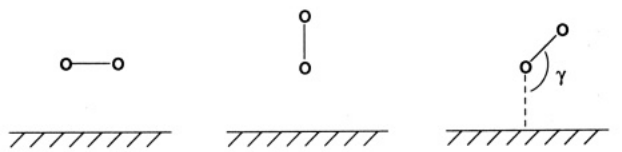

5 6 7

In experimental studies of monomeric dioxygen metal complexes, a linear or close to linear "end-on" coordination

(63) Gaspar, J. A.; Eguiluz, A. G.; Tsuei, K.-D.; Plummer, E. W. *Phys. Rev. Lett.* **1991**, *67*, 2854. Liebsch, A. *Phys. Rev. Lett.* **1991**, *67*, 2858, and references therein.

(64) Frank, K.-H.; Sagner, H.-J.; Heskett, D. *Phys. Rev. B* **1989**, *40*, 2767.

(65) Wyckoff, R. W. G. In *Crystal Structures*, 2nd ed.; Wiley-Interscience: New York, 1963; Vol. 1, p 14.

of dioxygen has not yet been found.[68] If O_2 is not side-on bonded to a metal center, it assumes a bent end-on position with γ typically in the range between 115 and 135°. Therefore, we limited out theoretical studies also to the side-on and bent end-on cases. The higher-symmetrical adsorption sites which we studied are illustrated in 8 for the side-on and in 9 for the end-on, mode.

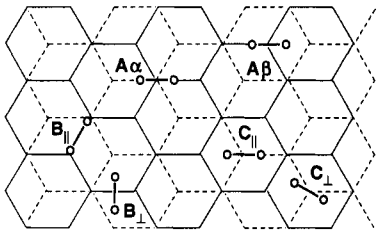

8

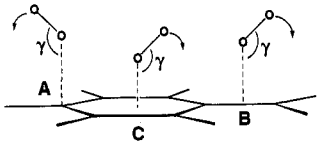

9

A refers again to on-top sites (α and β), **B** to sites over the center of a C–C bond, and **C** to sites over the center of a hexagon. Within these three basic sites one can descriminate further among various conformations. However, we elaborated on such conformational changes only for the side-on case. The most important difference occurs in the **B** site; we can have O–O aligned parallel to a C–C bond (eclipsed, or $\mathbf{B}_\parallel$ conformation) or perpendicular to it (staggered, $\mathbf{B}_\perp$). For the **C** site we can make a similar distinction ($\mathbf{C}_\parallel$ or $\mathbf{C}_\perp$, see 8). The conformational difference may be expected to be less pronounced in **A** and **C** compared to **B** sites, for the rotational barrier in **A** and **C** is 6-fold.

Instead of focusing on different conformations for the bent end-on mode we carried out a small angle-variation study (γ = 150, 135, and 120°) with the second oxygen approaching the surface as shown in **9**.

The O–O distance throughout most of our study was fixed at 121 pm—the separation in free O_2. While O_2 adsorption will surely result in lengthening of the O–O bond, the reason for one site being preferred over another should emerge more clearly if the O–O distance is kept fixed.

The choice of a suitable C–O distance is more problematic. In the absence of experimental studies of *chemisorbed* O_2 on graphite, we were left with theoretical studies of the process. We are aware of only one investigation of chemisorption of O_2 on a $C_{10}H_8$ (naphthalene) molecule in which C–O distances were optimized. Different methods give a C–O distance in the range of 129–142 pm for the chemisorption product (cf. Table 3 in ref 34). However, we feel that these values correspond to an optimized C–O *bond* and not to a C–O *distance* for chemisorbed O_2. 1,2-Dioxetanes[69–71] (**10**) or peroxiranes[69,71] (**11**) can be considered as molecular models for our O_2–graphite surface study. Depending on reaction path and method, a C–O separation of 176 and 200 pm, respectively, has been calculated for transition states for the ethylene–O_2 reaction.[69]

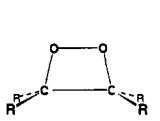

10

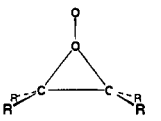

11

Subsequent studies showed us that we can take the region between 175 and 200 pm as appropriate for the C–O distance for O_2 chemisorbed on the basal graphite plane. (We use the word "chemisorbed" to indicate the regime of bond distances, where there is considerable C–O interaction, but do not mean to indicate that there necessarily is a chemisorbed state.) Table II compares the binding energy and O–O overlap populations for side-on chemisorbed dioxygen on graphite in different sites, assuming C–O distances of 150, 175, and 200 pm.

The calculated binding energies are all negative, indicating the endothermic character of the interaction. As anticipated, the Aα and β sites differ only very slightly. Having O–O lying above a C–C bond ($\mathbf{B}_\parallel$ site) seems to be the most likely side-on position. On the other hand, **C** sites and $\mathbf{B}_\perp$ are highly unfavorable. In all cases the O–O overlap population is lowered, compared to the free O_2 molecule, due to a filling of the dioxygen π^* level. A smaller overlap population should be accompanied by a lengthening of the O–O bond. The effect of C–O distance is such that at a longer separation of, e.g. 200 pm, the effects discussed here are essentially the same, albeit less pronounced. For instance, the binding energy is less negative. The increasingly negative binding energies at a shorter C–O distance of 150 pm underscore the 2-orbital/4-electron type repulsive interaction between O_2 and the graphite surface.

The respective values for the bent end-on approach in different sites and with different surface–O–O angles are compiled in Table III. While the **C** sites are again highly disfavored, the **A** position starts to become slightly exothermic. At a longer C–O separation (200 pm, results not reported here) **A** is even more exothermic and **B** also shows a positive binding energy. The angle variation is not very conclusive, its trend depending largely on the adsorption site. Again, for the bent end-on chemisorption, the O_2 π^* level lies below the Fermi energy.

The general trend that the binding energy becomes positive at larger distances from the surface is in agreement with the readily observed physisorption of dioxygen on graphite, with surface–adsorbate distances of the order of 300 pm.[34] On the other hand, dioxygen chemisorption on graphite is mostly an endothermic process. A bent end-on approach of the dioxygen molecule in the on-top site (**A**) is calculated as most favorable for real chemisorption. Here we note that graphite studies of O_2 indicate that there may not be such a thing as a chemisorbed O_2, but only physisorbed O_2,[32,48] since to our knowledge no molecular state except the physisorbed O_2 has ever been observed experimentally. We want to emphasize that the

(66) (a) Lorberth, J.; Shin, S.-H.; Wocadlo, S.; Massa, W. *Angew. Chem.* **1989**, *101*, 793; *Angew. Chem., Int. Ed. Engl.* **1989**, *28*, 735. (b) Jutzi, P.; Leffers, W.; Hampel, B.; Pohl, S.; Saak, W. *Angew. Chem.* **1987**, *99*, 563; *Angew. Chem., Int. Ed. Engl.* **1987**, *26*, 583. (c) Rabe, G.; Roesky, H. W.; Stalke, D.; Pauer, F.; Sheldrick, G. M. *J. Organomet. Chem.* **1991**, *403*, 11.

(67) (a) Janiak, C. *Chem. Ber.* **1993**, *126*, 1603. (b) Zerger, R.; Rhine, W.; Stucky, G. D. *J. Am. Chem. Soc.* **1974**, *96*, 5441.

(68) (a) Boca, R. *Coord. Chem. Rev.* **1983**, *50*, 1. (b) Gubelmann, M. H.; Williams, A. F. *Struct. Bonding (Berlin)* **1983**, *55*, 1. (c) Niederhoffer, E. C.; Timmons, J. H.; Martell, A. E. *Chem. Rev.* **1984**, *84*, 137.

(69) Hotokka, M.; Roos, B.; Siegbahn, P. *J. Am. Chem. Soc.* **1983**, *105*, 5263.

(70) Kopecky, K. R. In *Chemical and Biological Generation of Excited States*; Adam, W., Ed.; Academic Press: New York, 1982; p 85.

(71) Chen, C.-C.; Fox, M. A. *J. Comput. Chem.* **1983**, *4*, 488.

Table II. Comparison between Different Sites for Side-on Chemisorbed Dioxygen on Graphite as Illustrated in 8 at C–O = 150, 175, and 200 pm

				overlap population					
	E_b, binding energy/eV[b]			O–O[c]			C–O[d]		
site[a]	150	175	200	150	175	200	150	175	200
Aα	−7.82	−3.89	−1.23	0.492	0.469	0.470	0.104	0.045	−0.014
Aβ	−7.81	−3.88	−1.22	0.491	0.469	0.468	0.104	0.045	−0.014
$B_\parallel$	−4.15	−2.06	−0.17	0.531	0.493	0.488	0.404	0.233	0.026
$B_\perp$	−13.6	−6.49	−2.59	0.407	0.447	0.457	0.085	0.031	−0.001
$C_\parallel$	−10.5	−5.88	−1.84	0.627	0.597	0.551	0.337	0.201	0.045
$C_\perp$	−11.8	−7.04	−2.68	0.644	0.614	0.580	0.323	0.167	0.043

[a] See 8 for illustration, O–O was fixed at 121 pm. [b] $E_b = E$(bare graphite unit cell) + E(free O_2) − E(adduct) = (−2556.708 eV) + (−249.681 eV) − E(adduct). A positive binding energy indicates stabilization. [c] The overlap population in free O_2 with O–O = 121 pm is calculated as 0.793. [d] Overlap population between *one* carbon and *one* oxygen at the distance given. For the **A**, $\mathbf{B}_\parallel$, and $\mathbf{C}_\parallel$ sites there are two, for $\mathbf{B}_\perp$ and $\mathbf{C}_\perp$ there are four C–O contacts to consider for a relative measure of the O_2–graphite bond strength.

Table III. Comparison between Different Sites and Bending Angles for Bent End-on Chemisorbed Dioxygen on Graphite As Illustrated in 9 at C–O = 175 pm

			overlap population	
site[a]	surface–O–O angle, γ (deg)	E_b, binding energy/eV[b]	O–O[c]	C–O[d]
A[e]	150	0.143	0.462	0.238
	135	0.245	0.481	0.253
	120	0.113	0.495	0.266
B	150	−0.400	0.468	0.193
	135	−0.442	0.480	0.190
	120	−0.833	0.487	0.181
C	150	−10.30	0.530	−0.007
	135	−11.10	0.527	−0.033

[a] See 9 for illustration, O–O was fixed at 121 pm. [b–d] See notes on Table II. [e] Because of the close similarity between α and β sites, no distinction is made anymore.

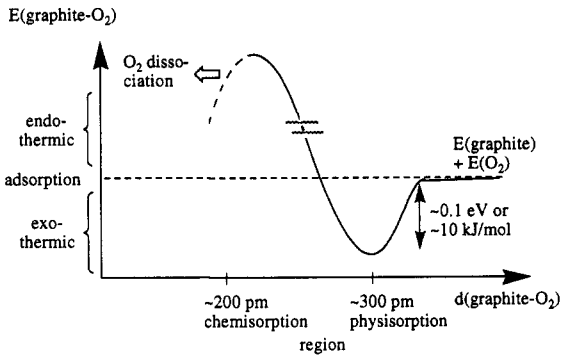

Figure 4. Schematic representation of the energetics of the graphite–dioxygen interaction. Physisorption is intended to mean a van der Waals interaction while chemisorption should describe a chemical (orbital) interaction. Physisorption energies are generally in the 0.1-eV range, also for O_2 on graphite.[43] Approximate distances are from ref 34.

results clearly demonstrate that there is no stable state for O_2 chemisorption. At most, the molecule may only be trapped in a weakly bound state for a limited time. In this respect O_2–graphite is very much like H_2 on Cu[72] and H_2 on Mg.[73] The van der Waals interaction is probably the dominant attractive term for O_2 interacting with clean graphite. We define *physi*sorption as a mere van der Waals interaction, while *chemi*sorption in our nomenclature is intended to mean a chemical (orbital) interaction, i.e. a shift in electron density. Figure 4 summarizes what we extract as the common, accepted picture concerning the energetics of O_2 *chemi-* and *physi*sorption on graphite.

The preference for the **A** site for bent end-on or the $\mathbf{B}_\parallel$ site for side-on bonding derives, we think, from the fact that in these positions O_2 interacts with the least number of carbon atoms and requires only the formation of four-coordinated carbon atoms in reasonable geometries. The **A** site for the side-on mode presents also an interaction with one carbon atom only, but it makes this carbon atom five-coordinated.

If we allow for a synergistic simple distortion or reconstruction around the interacting carbon atom(s), such that the atoms involved are slightly elevated above the graphite plane (**12**, **13**), the O_2 binding energies increase somewhat, even after correcting from the reconstruction energy. An elevation of d = 50 pm above the surface corresponds to almost tetrahedral angles around carbon.

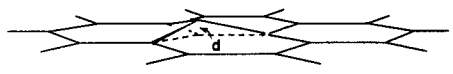

12

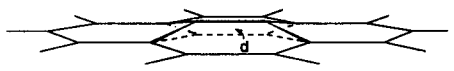

13

For a small reconstruction (d = 25 pm) the gain in binding energy is largest (0.6 eV more for **A**, bent end-on; 1 eV more for $\mathbf{B}_\parallel$, when compared to the undistorted case). The experimentally observed low sticking coefficient for O_2 (at temperatures higher than 50 K)[32,48] suggests that the resulting energy for the distored **A** site is still not large enough to trap an O_2 molecule effectively in a chemisorbed state (because kT is too large in comparison with the well depth). Potassium facilitates the distortion only (and to a very limited amount) if the elevated carbon atom is part of the hexagon above which the alkali metal sits. With potassium close by, the energy required for the distortion decreases by about 0.1 (d = 25 pm) to some 0.4 eV (d = 50 pm).

Oxygen Atoms on Graphite. The experimental findings point to a difference in reactivity between a dioxygen *molecule* and an oxygen *atom*. We need to examine theoretically oxygen *atoms* on a graphite surface, to check if pronounced differences do indeed exist. We start again with a comparison between different sites (cf. **9**) for chemisorbed monooxygen on graphite. The results are compiled in Table IV.

For the **A** and **B** site we find rather large positive binding energies (indicating stabilization) with the on-top site being slightly favored over the bridging site. The **C**-site or 6-fold hollow position can be excluded immediately. The stabilizing chemisorption energies for an O-atom at a C–O distance used before for dioxygen correlate with our expectations. It makes chemical sense that one obtains a "stable" chemisorption adduct from a highly reactive species such as monooxygen.

(72) Harris, J.; Andersson, S. *Phys. Rev. Lett.* **1985**, *55*, 1583.
(73) Nørskov, J. K.; Haumöller; Johansson, P. K.; Lundquist, B. I. *Phys. Rev. Lett.* **1981**, *46*, 257.

We can further justify the formation of gaseous oxidation products (CO, CO_2) from the monooxygen chemisorption, since the C–C overlap population of the adjacent bonds drops significantly from 1.016 for clean graphite to 0.877 for O in the on-top site. This difference in C–C overlap population becomes even larger if we distort the interacting carbon by elevating it 25 or 50 pm above the surface (cf. **12**). With O on-top, the C–C overlap population to its neighbors decreases to 0.33 in both cases—down from 0.91 (50 pm above surface) to 0.99 (25 pm elevation) for the clean distorted graphite. At the same time the binding energy for monooxygen increases.

We may add that experimentally it would be of interest to explore the branching ratio $CO:CO_2$, when only atomic oxygen is present on the surface. As far as we know, these ratios $O_2:CO:CO_2$ for atomic oxygen (no potassium) on the surface have not been measured. With K on the surface there is only negligible CO and O_2 desorption.[44] It would be of interest to deposit atomic oxygen, followed by measurement of the $O_2:CO:CO_2$ ratios.

Reactivity of Defects in the Graphite Surface. Microscopic techniques such as STM[74] and etch-decoration transmission electron microscopy as well as scanning electron microscopy[41,75] show clearly the formation of monolayer pits on graphite upon its gasification reaction with atomic and molecular oxygen. It is proposed that these pits start at existing defects (e.g. atomic vacancies) and can be readily expanded with atomic oxygen at about 150 °C at a rate which is several times faster than the oxidation rate in molecular oxygen at 650 °C.[40] Although some expansion of the pits with O_2, after preceding O atom exposure, is apparently possible, its extent is not clear. Work on graphite gasification by molecular oxygen is usually carried out at elevated temperatures (650 °C and above), where O_2 can thermally dissociate. It is quite possible that at these temperatures sufficient atomic oxygen is formed to dominate the reaction.[41]

In our own experimental work, we also observed a reaction-induced etch pit at the center of one sample that had been used extensively in reactive experiments. We suspect that a cooperative effect of the electron beam (with energy up to 10 keV), and reactions involving coadsorbed K and O_2, was responsible for the pit formation.

We tested the influence of an atomic defect, i.e. a C vacancy on the basal graphite surface, by first removing a single carbon atom (from an α site) and then adsorbing a dioxygen molecule (bent end-on), or an oxygen atom, above the vacancy (**14**).

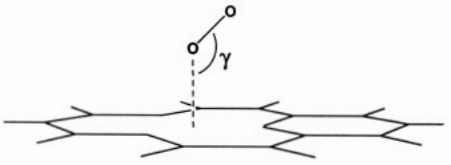

14

The binding energy for a vacancy with O adsorbed right above it indicated only a minor improvement, while for O_2 it was even less favorable compared to the defect-free surface. The O–O and C–O overlap populations also do not give a clear indication whether a single atom vacancy will facilitate the sticking and dissociation of an O_2 or O adsorbate.

Such a small effect on a surface defect worried us at first, especially so in light of recent STM studies that indicate the ready formation of larger pits on preexisting defects by heating highly pyrolytic graphite samples in air at 650 °C.[76] We then tried to derive an understanding of the frontier orbitals—the dangling bonds—with the use of a molecular model. A look at the molecular orbitals of **15** in comparison to **16** showed that the unsaturated σ levels are raised in energy—but so are the π levels. There is a concentration of electron density on the carbenoid carbons, but σ is still substantially below the π level (see **17**).

Table IV. Comparison between Different Adsorption Sites for Monooxygen on Undistorted Graphite at C–O = 175 pm

		overlap population	
site	E_b/eV[a]	C–O	C–$C_{closest}$
A[b]	+3.10	0.231	0.877
B	+2.28	0.187	0.756 (bond underneath O)
C	−8.68	−0.007	0.912

[a] $E_b = E$(graphite unit cell) + E(free O) − E(adduct). A positive binding energy indicates an exothermic adsorption process. [b] Because of the close similarity between α and β sites, no distinction is made between these.

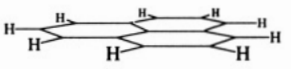

15

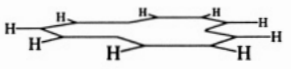

16

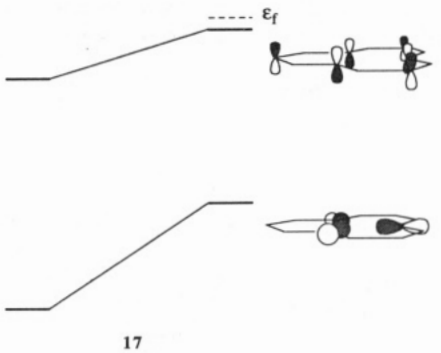

17

The symmetry plane of the molecule prevents mixing between σ and π dangling bonds, so that there is little electron density in the region *above* the vacancy. However, things are slightly more complicated, as shown by a theoretical study which was carried out by Soto on graphite (one or two layer slab, extended Hückel tight-binding method) with a single atom vacancy.[77] The results indciate a distance dependence of the charge density directly above the vacancy. This is explained by the localized nature of the nonbonding crystal orbitals from the nearest neighbor atoms to the vacancy. In the calculated STM image the vacancy would appear as a "hole" only at low altitudes, whereas it would look like a maximum or "bump" at high altitudes, with the changeover occurring at an altitude of about 175 pm. From the orbital pictures in **17** we could expect a more pronounced defect influence if we had the O_2 or O-adsorbate approach the defect site either above the rim or in the surface plane—as indicated in **18**.

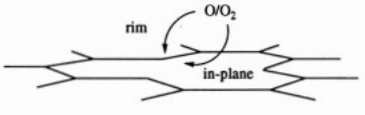

18

We thus explored putting dioxygen and monooxygen on top of a rim atom (**19**) and—after removing a second

(74) Chang, H.; Bard, A. J. *J. Am. Chem. Soc.* **1990**, *112*, 4598.
(75) Walker, P. L., Jr. *Carbon* **1990**, *28*, 261.
(76) Chang, H.; Bard, A. J. *J. Am. Chem. Soc.* **1991**, *113*, 5588.
(77) Soto, M. R. *J. Microsc.* **1988**, *152*, 779.

carbon atom—in the plane of the surface layer (**20**). Adsorbing O or O_2 *in the plane* of the graphite surface *with one vacancy only* would require C–O distances of 142 pm! We therefore decided to remove a second carbon atom which creates a large enough vacancy to accommodate an O atom with C–O = 175 pm.

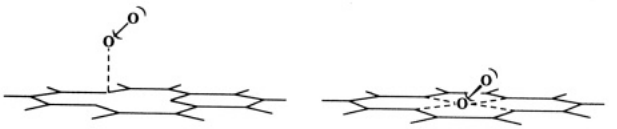

19 20

Note that the in-plane approach, modeled in **20**, results in simultaneous interactions with four carbon atoms with dangling bonds. For the rim position, (**19**) we find binding energies which are about 1.5 eV more positive than the respective values for the undamaged graphite surface. For the in-plane approach **20** the binding energies are smaller by more than 2 eV, which we, however, attribute to the square-planar environment for the oxygen atom.

Actually, we would expect a larger positive energy of chemisorption for the in-plane trajectory than for the rim-site, because of the localized nature of the dangling σ orbitals (versus π) and their better energy match with the (di)oxygen levels. Therefore, to model a more reliable in-plane approach, we had to extend the pit even further. This could only be done by resorting to an even larger unit cell of 24 carbon atoms for the surface layer (plus 32 atoms for an eventual second layer), shown in **21**.

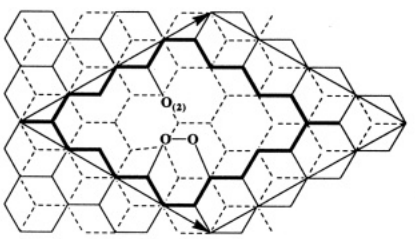

21

Indeed, for this large enough defect we find in-plane binding energies which are an additional 2–3 eV more positive than for the respective rim-position. We carried out these calculations using a one- (defect surface only) and two-layer (see **21**) slab. From our computational parameters we fail to see any effect on the second layer, with respect to which dioxygen is then in the physisorption range. Experimentally, the physisorption binding energy is found to be rather small, only ~0.1–0.2 eV.[43]

We note that surface defects (one to multiatom vacancies, **14**–**21**) also have a stabilizing effect for potassium atoms. The binding energies for potassium adsorbed on top of a rim atom (cf. **19**), or over a vacant site (cf. **14**), or in an in-plane position (cf. **21**) such that C–K = 303 ppm, are some 0.2–0.5 eV stronger than for respective positions on the undamaged surface. This is consistent with the large increase in desorption temperature for potassium from an argon bombarded (and thus damaged) surface.[44]

Potassium–Dioxygen Coadsorption. We have now set the stage for an investigation of potassium–dioxygen coadsorption on a graphite surface. There now enters a new parameter, the K–O_2 separation, in addition to the already mentioned different possible adsorption sites for potassium and dioxygen. The schematic drawing in **22** illustrates what is meant; having potassium in a 6-fold hollow (**C**) site and dioxygen coadsorbed, e.g. above a C–C bond ($\mathbf{B}_\parallel$ site), allows for four different K–O_2 chemisorption patterns, which differ in their K–O_2 separation and relative orientation (taking into account the potassium atoms in the neighboring unit cells). The same is true for dioxygencoadsorbed in the bent end-on position above a C-atom (**A** site). With the freedom of O–O rotating about the C···O contact, we even have various conformations in addition to three different K/O_2 chemisorption patterns (**23**). However, for simplicity we calculated only three conformers with the second O-atom above a C–C bond, as shown in **23**.

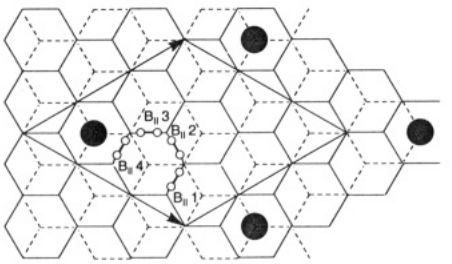

22

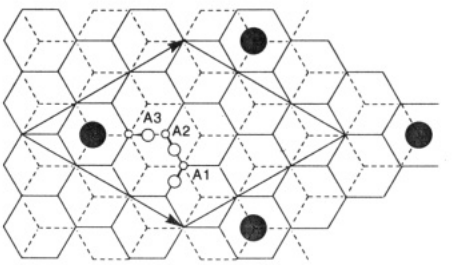

23

Furthermore, we can envision an entirely new chemisorption site for the oxygen molecule when it is brought onto the potassium/graphite surface: O_2 can sit above a preadsorbed K atom, either side-on (**24**) or bent end-on bonded (**25**). These adsorption sites will be denoted **K1** and **K2**, respectively.

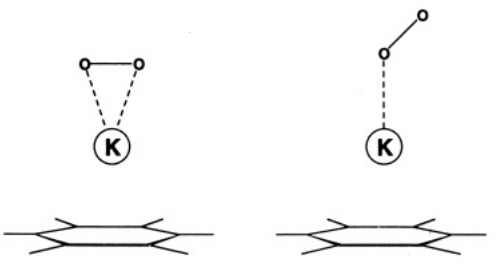

24 25

For these sites the K–O distance was fixed at 270 pm, based on a comparison to the inorganic complexes $K[C_5(NO_2)_2Cl_3]$[78] (K–O ≈ 258–294 pm), $K[C_5(CO_2Me)_5]$-(MeOH)[79] (K–O ≈ 264–288 pm), and $[(PhCH_2)_5C_5]K$-$(OC_4H_8)_3$[66] (K–O ≈ 269–278 pm).

In Table V we compare different potassium–dioxygen chemisorption patterns with respect to the dioxygen binding energies, O–O and K–O overlap populations. The potassium position was fixed in the **C** site (K–C = 303 pm,

(78) Otaka, Y.; Marumo, F.; Saito, Y. *Acta Crystallogr. B* **1972**, *28*, 1590.

(79) Bruce, M. I.; Walton, J. K.; Williams, M. L.; Hall, S. R.; Skelton, B. W.; White, A. H. *J. Chem. Soc., Dalton Trans.* **1982**, 2209.

Table V. Comparison between Different Potassium–Dioxygen Chemisorption Patterns on Graphite at C–O = 175 pm

O_2 site[a]	K–O distances/pm	E_b, binding energy/eV[b]	overlap population O–O[c]	overlap population K–O
	Side-on, See **22**			
$B_{\|}1$	385/385	−1.66	0.501	0.009
$B_{\|}2$	297/374	−1.32	0.504	0.095/−0.009
$B_{\|}3$	167/282	+0.18	0.521	0.346/−0.052
$B_{\|}4$	153/153	+1.20	0.543	0.209
	End-on, See **23** (135° C–O–O tilt angle)			
A1	387/369	+1.14	0.479	0.002/0.022
A2	299/335	+1.38	0.486	0.078/0.008
A3	170/228	+2.88	0.522	0.230/0.054
	Above Potassium Atom, See **24** and **25**			
K1	270/270	+6.35	0.483	0.075
K2	270/366	+6.13	0.465	0.193/−0.026

[a] O–O was fixed at 121 pm. [b] $E_b = E$(carbons + potassium) + E(free O_2) − E(surface/adsorbate complex). A positive binding energy indicates an exothermic adsorption process. [c] The overlap population in free O_2 with O–O = 121 pm is calculated as 0.793.

see above). We include only dioxygen sites (except for the novel **K** sites) which were found to be most likely from our O_2/graphite calculations, namely the $\mathbf{B}_{\|}$ site for side-on and the **A** site for end-on chemisorbed O_2. The sites deemed unlikely from our earlier calculations remain so, even with potassium as a coadsorbate.

For dioxygen in the $\mathbf{B}_{\|}$ and **A** sites we note the strong shift of the binding energy toward more positive values, indicating the increased exothermic character of the O_2 adsorption on a graphite surface with a preadsorbed potassium layer. In other words, the energy lowering upon impingement of an O_2 molecule on the surface (as one condition for sticking) is enhanced drastically by a potassium coadsorbate. The closer the oxygen approaches a potassium atom, the stronger the binding energy becomes.

The large binding energies for the **K** sites (dioxygen on top of potassium) are striking. They surpass the comparable values for all other chemisorption patterns by more than 3 eV. Moreover, the stabilization provided by potassium for the O_2 chemisorption (in the **K** site) is still some 1.5–2 eV higher than the already sizable stabilization derived from defects in the graphite surface (in-plane approach of O_2; **21**, E_b = 4.10 eV end-on; 4.64 eV side-on). In the following we try to rationalize the local nature of the potassium enhancement with the help of molecular models. But before we do so, we would like to show that at our level of computation, molecular models preserve the trends seen from the investigation of extended structures. Table VI compiles some molecular systems and compares binding energies and overlap populations to the values in analogous extended structures.

Even though Table VI presents a very brief list, one realizes that the overlap populations tend to be surprisingly similar in molecular and extended systems. The binding energy values may vary a little bit, but the trend in stabilization upon going from side-on bonded O_2, over bent end-on, to O_2 above a potassium, is clearly preserved.

If we now examine the interaction diagrams between O_2 and the molecular C_n fragments (not shown here), we note some subtle differences in the orbital interactions: For O_2 side-on bonded to $C_{16}H_{10}$ we have a very strong perturbation of the carbon π system through a repulsive O_2 π^*/C π interaction. Such a repulsive interaction gives rise to the destabilization of side-on adsorbed O_2 on graphite (see above). For O_2 end-on bound to $C_{16}H_{10}$, on the other hand, the repulsive O_2 π^*/C π interaction is rather weak and a 2-orbital/2-electron O_2 σ/C_n π interaction becomes predominant with a smaller carbon π-level perturbation.

When O_2 is adsorbed on top of a potassium, sitting in turn above a C_6H_6 ring, one sees only a very small perturbation for the benzenoid π system and the O_2 π^* level—illustrated in Figure 5. We see again an important role of the O_2 σ and O_2 π orbital as they interact with the potassium s–p hybrid. It is this hybrid pointing away from the surface which mediates the sticking and *chemical* interaction of O_2 with the graphite surface at a C–O distance which is normally in the physisorption region. The large positive binding energy for O_2 on top of the potassium can be traced to the transfer of the remaining electron density on potassium into the O_2 π^* level.[5]

Dioxygen Dissociation. It is generally accepted that the gasification of graphite is preceded by chemisorption (sticking) of the dioxygen molecule on the surface, followed by its dissociation to oxygen atoms. In our investigation we emphasized the (dissociative) sticking component as the apparent bottleneck in the reaction process. And indeed, as the O–O overlap population in all of the tables shows, the O–O bond strength is substantially lowered when the dioxygen molecule interacts with the surface—even in cases with a negative binding energy. From much experience a lowered overlap population correlates with a weaker bond. Thus, a lengthening of the O–O bond should occur. This may eventually lead to bond dissociation. Let us explore this dissociation in some more detail.

Figure 6 shows the Walsh diagram (orbital energies versus atomic separation) for the O–O bond stretch in a free dioxygen molecule. The left-hand value on the abscissa—121 pm—is the equilibrium distance in free O_2. The doubly degenerate π^* level is half filled with two electrons, giving rise to the well-known paramagnetic character of dioxygen in its triplet $^3\Sigma_g^-$ ground state.

The lowering of the overlap population upon chemisorption stems from the filling of the antibonding π^* level. The oxygen π^* (at about −13 eV) lies below the Fermi level of the graphite slab, around −11 eV. One has, of course, to be careful here since in our simple one-electron approximation the O_2 π^* would be filled even at large separation from the surface. However, if one is in a region where adsorbate–substrate interaction is likely to occur (cf. C···O = 200 or 175 pm), we may rely on these results.

Putting two more electrons into an antibonding orbital will, of course, weaken the corresponding bond. Occupying the π^* level in O_2 ($\rightarrow O_2^{2-}$) is not yet, by itself, sufficient to break the bond. With the overlap population dropping from 0.79 to ca. 0.46–0.50 (cf. Tables II–VI) the atoms can still be consided to be held together by the σ bond. However, from molecular dioxygen–metal complexes it is known that as the number of antibonding electrons rises from O_2 through O_2^- to O_2^{2-} the O–O distance increases from 121 over 133 to 149 pm[80] (accompanied by a distinct lowering of the O–O stretching frequency). As pointed out above, such a bond lengthening—possibly to approximately 150 pm, depending on the adsorption site—will also occur with dioxygen on the graphite surface.

Returning now to Figure 6 we realize that the strongly antibonding σ^* level experiences a dramatic decrease in energy upon lengthening of the O–O bond. Our qualitative calculations show that the energy of σ^* approaches the Fermi level of the surface at an O–O separation of about 150–160 pm. Once it sinks below the Fermi energy (ϵ_f) it will be filled by two electrons from the slab (**26**), giving rise to a dissociation of the molecule into oxygen atoms.

An additional experiment to test for chemisorbed active monooxygen may be the use of carbon monoxide as a reducing material. A recent study indicated that the

(80) Vaska, L. *Acc. Chem. Res.* **1976**, *9*, 175.

Table VI. Comparison between Molecular Surface–Adsorbate Models and the Analogous Extended Structure System

	molecular system			analogous extended structure		
		overlap population			overlap population	
	E_b[a]	O–O	C–O	E_b[a]	O–O	C–O
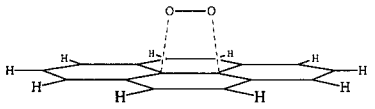	−2.18	0.49	0.24	−2.06	0.49	0.23 (cf. Table II, $B_{\|}$)
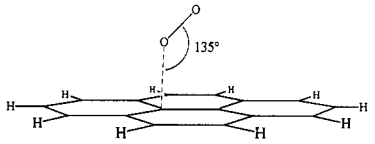	−0.08	0.48	0.26	+0.25	0.48	0.25 (cf. Table III, A, 135°)
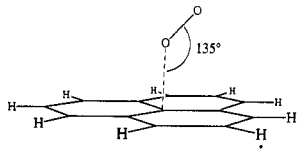	−0.06	0.48	0.26	+0.25	0.48	0.25
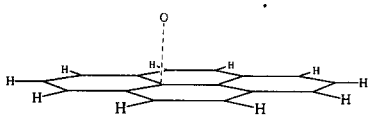	+2.75		0.87	+3.10		0.88 (cf. Table IV)
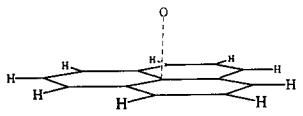	+2.77		0.87	+3.10		0.88

	molecular system			analogous extended structure		
		overlap population			overlap population	
	E_b[a]	O–O	K–O	E_b[a]	O–O	K–O
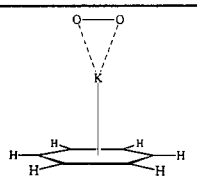	+5.00	0.51	0.08	+6.35	0.48	0.08 (cf. Table V, K1)
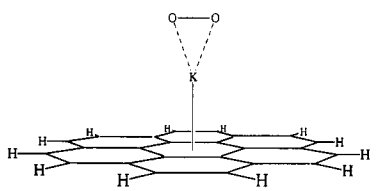	+5.94	0.48	0.08	+6.35	0.48	0.08

[a] $E_b = E$(substrate) + E(free O/O_2) − E(adduct). A positive binding energy indicates an exothermic adsorption process.

oxidation of CO may be used as a probe reaction to detect some forms of chemisorbed oxygen in coals.[81]

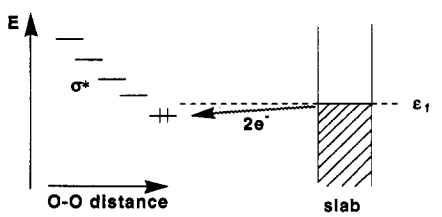

26

We have focused here on the O_2 dissociation step, since it seems to be the more important rate limiting step in CO and CO_2 formation of graphite. We did not explore in any detail the C–O bond formation nor the detachment of CO/CO_2 from the surface. Also left for a later study are the formations of K–O and K–C–O complexes on the surfaces and their likely stoichiometries.

Theoretical Conclusions

Supplementing the experimental results, we have tried to provide a possible understanding of parts of a graphite gasification mechanism, especially the dioxygen adsorption and dissociation. We attempted to work out the differences between O_2 adsorption on clean or potassium-covered graphite in a chemical, molecular orbital picture.

We found that in the absence of potassium on the surface there is no deep potential energy well in O_2 chemisorption, allowing only physisorption of O_2 molecules with low kinetic energy.[32] A deep potential minimum developes only for oxygen atoms. However, experimentally this requires substantial kinetic energy input in the appropriate degrees of freedom (translational, vibrational and/or rotational energy), either by raising the temperature or providing the O_2 with kinetic energy using molecular beam techniques to overcome the $O_2 \rightarrow 2O$ dissociation barrier. With potassium on the surface this dissociation barrier is

(81) Hinckley, C. C.; Wiltowski, T.; Wiltowska, T.; Ellison, D. W.; Shiley, R. H.; Wu, L. *Fuel* **1990**, *69*, 103.

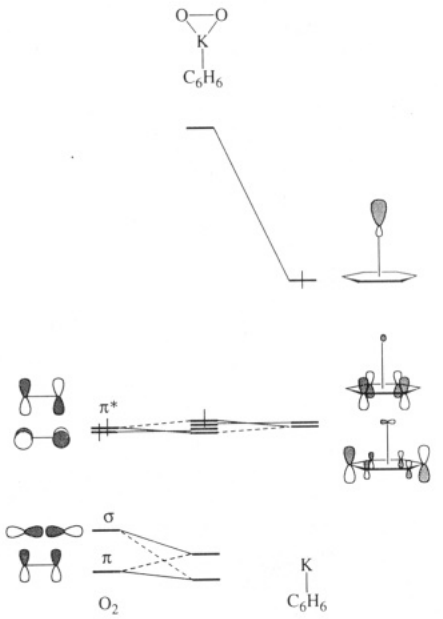

Figure 5. Partial interaction diagram for dioxygen bonded side-on to a benzene–potassium fragment (**K1** site). Lack of perturbation of the benzenoid π system together with a good overlap between the dioxygen σ and π level and a potassium sp hybrid explains the large energy of interaction. A vertical bar indicates the occupation of the HOMO.

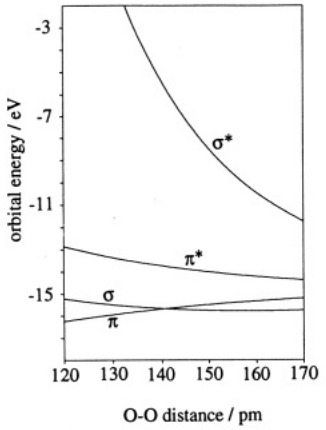

Figure 6. Partial Walsh diagram for the stretching of the O–O bond in the dioxygen molecule. 121 pm is the medium distance in free O_2. The doubly degenerate π^* level is the half-filled, highest occupied MO.

significantly reduced due to the destabilization of the O–O bond, caused by charge transfer from potassium to antibonding O_2 orbitals.

We suggest the following "dynamic" picture of O_2 approaching K-graphite: As O_2 approaches a K atom, it first fills π^* which leads to a bond length increase, which in turn shifts σ^* down until it falls below ϵ_f. Then σ^* becomes populated and the O–O bond weakens drastically until dissociation occurs. We see the potassium promotion effect as a very local one, in that the alkali strongly facilitates the chemisorption of dioxygen with formation of a K–O_2 surface complex. The promoter effect of potassium surpasses that of surface defects and distortions. The potassium catalyst's role can be described as enabling the sticking of O_2 and subsequent dissociation on graphite at a surface···O_2 distance where normally only physisorption occurs. A potassium s–p hybrid pointing away from the surface—together with no endothermic disturbance in the graphite π system—provides for the stabilizing K–O_2 interaction. For atomic monooxygen we find the expected stabilizing chemisorption already with no potassium present.

Acknowledgment. C.J. thanks the Deutsche Forschungsgemeinschaft (DFG) for the award of a postdoctoral and a Habilitation fellowship. The theoretical work carried out by C.J. initiated during a postdoctoral stay at Cornell in the group of R.H. and was finished upon return to Berlin. At Cornell our work was supported by the Office of Naval Research and the National Science Foundation through the Materials Science Center at Cornell, Grant DMR-9121654. The TU Berlin is thanked for providing computer time, the "Fonds der chemischen Industrie", and the "Freunde der TU" for additional support.

We thank John Lowe for helpful suggestions and for bringing some of the theoretical work on graphite to our attention and one of the reviewers for his or her very constructive comments. Furthermore, we are grateful to Dinko Chakarov for valuable discussions and for help with the HREELS measurements.

Appendix

The computations were performed within the extended Hückel formalism[82] with weighted H_{ij} values.[83] The atomic parameters for the elements involved in our calculations were as (H_{ii}, ζ): C 2s, −21.4 eV, 1.625; 2p, −11.4 eV, 1.625;[82] O 2s, −32.3 eV, 2.275; 2p, −14.8 eV, 2.275;[82] K 4s, −10.49 eV, 1.2; 4p, −7.37 eV, 1.2; from charge iteration, see text. The parameters for the charge iteration of the potassium atom were A = 1.00304/1.34340; B = 6.63321/4.49320; C = 4.30229/2.72900. Geometrical parameters and k-point sets are referred to in the appropriate tables or in the text. The intralayer C–C distance in the undistorted graphite net was fixed at 142 pm, the interlayer contact at 335 pm.

Chosing the Brillouin Zone and k-Point Set. Our bare graphite slab in **3** still has 3-fold symmetry. Together with the inversion symmetry of the Hückel Hamiltonian the irreducible part of the Brillouin zone is $^1/_{12}$ of the full zone. However, bringing in an adsorbate, such as potassium or O_2, above a C–C bond, already reduces the symmetry to 2-fold, with the irreducible Brillouin zone (IBZ) then occupying one-quarter of the full first Brillouin zone (**27**).[37] Coadsorption of K and O_2 (**28**) may leave no symmetry at all, thus giving only an oblique coadsorbate/substrate unit cell.

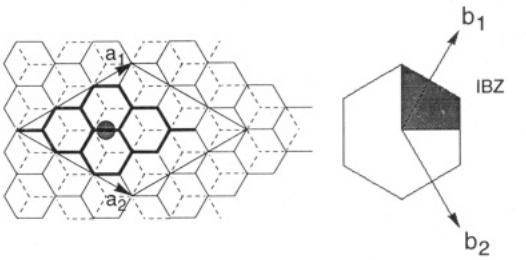

27

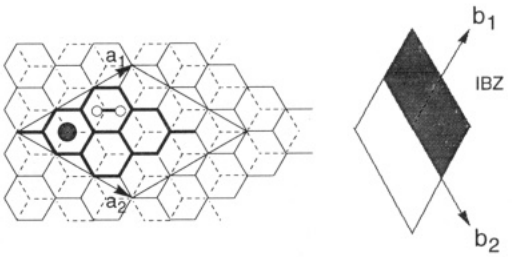

28

For the special case of an oblique lattice with $\angle a_1a_2$ = 60° and $\angle b_1b_2$ = 120°, respectively, the unit cell in reciprocal

space of the oblique lattice corresponds to the full Brillouin zone (BZ) of the hexagonal lattice, as depicted in **29**. The shaded or lined areas of the oblique BZ can be mapped onto an area of the hexagonal lattice by means of an inversion center (O). Therefore, there is no problem in using the k-point sets for an oblique lattice also in cases of higher hexagonal symmetry. Actually, even in 6-fold symmetrical hexagonal lattices it is safer to average over the whole BZ (shown in **29**) instead of just the irreducible BZ (given in **2**), to ensure a reliable calculation of properties.

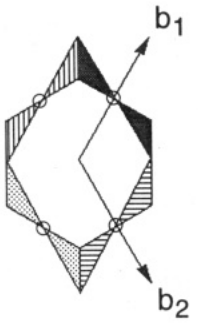

29

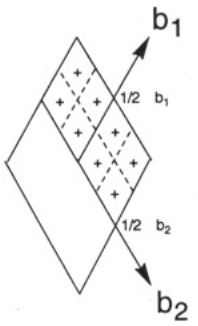

30

In order to be consistent in average property calculations, and to be able to compare results for different systems, one has to use the same k-point set for both low- and high-symmetry systems. Due to computational constraints, we decided on using a grid with only eight k-points—though a highly efficient one[84]—shown in **30** (the k-points are indicated by + − labels), throughout our average property calculations. The efficiency of the small k-point set in **30** was verified through a comparative average property calculation on graphite using 18 and 72 k-point sets.

The Potassium Parameters. The parameters of the extended Hückel method are the Coulomb integrals H_{ii} and Slater orbital exponents ζ. The choice of these for systems spanning a range of ionic and covalent bonding is always a problem. For carbon and oxygen there exist well-established literature parameters. However, taking a set of potassium parameters for neutral K, which we found in the literature (H_{4s} = −4.34 eV, H_{4p} = −2.73 eV, $\zeta_{4s,4p}$ = 0.87[85]) creates serious problems, as it gives rise to strong counterintuitive mixing (COM) in our semiempirical calculations. COM has been described before, and the conditions for its occurrence were analyzed in detail.[83,86] We just mention briefly the features of this phenomenon in our problem. The effect is easiest illustrated by using a molecular model for our extended surface system.

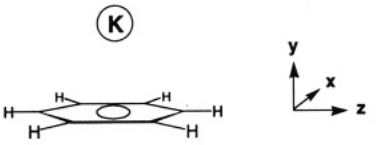

31

If we carry out a molecular calculation on a neutral benzene–potassium model (**31**) using the potassium parameters given above and a reasonable C–K distance of 303 pm (see above), we compute an atomic charge on potassium of +1.21 (!), a K–C overlap population of −0.08, and gross atomic orbital populations for the potassium s, y, and x/z orbitals of −0.05, −0.13, and −0.01, respectively (despite using the weighted Wolfsberg–Helmholtz formula[83]). A calculation with potassium on the extended graphite surface gives very similar values. These unrealistic values can be attributed to the above mentioned counterintuitive orbital mixing—the out-of-phase admixture of an energetically high-lying metal orbital into a very low lying ligand combination.[83,86] In our case the main interaction responsible for COM takes place between the potassium p_y and the benzene all-bonding, a_1 carbon 2s combination—graphically illustrated in **32** (the numbers denote the orbital energies in eV). To a smaller extent the potassium s orbital is also involved.

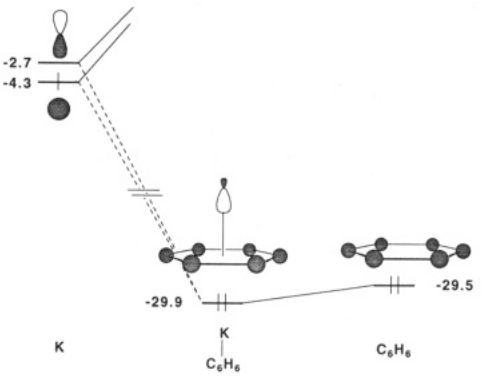

32

The potassium y and s orbitals overlap substantially with the C_6H_6 a_1 combination (overlap matrix element −0.56 for y and 0.40 for s), while they differ much in ionization potentials (see **32**). These are the conditions leading to COM within the extended Hückel framework.

To obtain a better set of parameters, we therefore performed a charge iteration on potassium on an extended graphite surface. For the charge iteration the potassium–graphite geometry was kept constant with C–K = 303 pm and potassium placed above a 6-fold site at 0.4 ML coverage (1K/18C atoms). A one-layer graphite surface had to be used in the charge iteration procedure, due to computational constraints. In addition we carried out charge iterations for different exponents ($0.87 < \zeta_{s,p} < 1.40$) to find an optimum parameter set which would give a small positive C–K overlap population and a potassium charge as close to +1 as possible, yet still having diffuse potassium orbitals ($\zeta_{4s,p}$ as small as possible). The set with an exponent $\zeta_{4s,p}$ = 1.20 with H_{4s} = −10.49 and H_{4p} = −7.37 eV was then our final choice and the basis for the subsequent calculations involving potassium on graphite.

(82) (a) Hoffmann, R. *J. Chem. Phys.* **1963**, *39*, 1397. (b) Hoffmann, R.; Lipscomb, W. N. *J. Chem. Phys.* **1962**, *36*, 2179; **1962**, *37*, 2872. (c) Whangbo, M.-H.; Hoffmann, R.; Woodward, R. B. *Proc. R. Soc. London, Ser. A* **1979**, *366*, 23.

(83) Ammeter, J. H.; Bürgi, H.-B.; Thibeault, J. C.; Hoffmann, R. *J. Am. Chem. Soc.* **1978**, *100*, 3686.

(84) Ramirez, R.; Böhm, M. C. *Int. J. Quantum Chem.* **1988**, *34*, 571.

(85) Alvarez, S.; Mota, F.; Novoa, I. *J. Am. Chem. Soc.* **1987**, *109*, 6586.

(86) Whangbo, M.-H.; Hoffmann, R. *J. Chem. Phys.* **1978**, *68*, 5498.